Thiolate Ligation of the Active Site Fe^{2+} of Isopenicillin N Synthase Derives from Substrate Rather Than Endogenous Cysteine: Spectroscopic Studies of Site-Specific Cys → Ser Mutated Enzymes†

Allen M. Orville,‡ Victor J. Chen,*,§ Aidas Kriauciunas,§ Mark R. Harpel,‡,∥ Brian G. Fox,⊥ Eckard Münck,⊥ and John D. Lipscomb*,‡

Department of Biochemistry, Medical School, University of Minnesota, Minneapolis, Minnesota 55455, Lilly Research Laboratories, Indianapolis, Indiana 46285, and Department of Chemistry, Carnegie Mellon University, Pittsburgh, Pennsylvania 15213

Received December 18, 1991; Revised Manuscript Received February 28, 1992

ABSTRACT: Isopenicillin N synthase (IPNS) catalyzes double ring closure of the tripeptide (L-α-amino-δ-adipoyl)-L-cysteinyl-D-valine (ACV) to form the β-lactam and thiazolidine rings of penicillin-type antibiotics. Our previous spectroscopic study using IPNS from *Cephalosporium acremonium* expressed in *Escherichia coli* [Chen, V. J., Orville, A. M., Harpel, M. R., Frolik, C. A., Surerus, K. K., Münck, E., & Lipscomb, J. D. (1989) *J. Biol. Chem. 264*, 21677–21681] indicated that a thiolate enters the coordination of the essential active site Fe^{2+} when ACV binds to IPNS. The presence of an Fe–S bond in the IPNS·ACV complex is confirmed by EXAFS data presented in the preceding paper [Scott, R. A., Wang, S., Eidsness, M. K., Kriauciunas, A., Frolik, C. A. & Chen, V. J. (1992) *Biochemistry* (preceding paper in this issue)]. However, these studies leave unclear whether the coordinating thiolate derives from ACV or an endogenous cysteine. Here, we examine the spectroscopic properties of three genetically engineered variants of IPNS in which the only two endogenous cysteines are individually and collectively replaced by serine. The EPR, Mössbauer, and optical spectra of the mutant enzymes and their complexes with ACV, NO, or both ACV and NO are found to be essentially the same as those of wild-type IPNS, showing that the endogenous cysteines are not Fe^{2+} ligands in any of these complexes. Spectral quantitations show that the double Cys → Ser mutation decreases the affinity of the enzyme for ACV by about 6-fold, suggesting that the endogenous cysteines influence the structure of the substrate binding pocket remote from the iron. Thiolate complexation of the Fe^{2+} is also examined using ACV analogues. All ACV analogues examined in which the cysteinyl thiol moiety is unaltered are found to bind to the IPNS·NO complex to give optical and EPR spectra very similar to those of the ACV complex. In contrast, analogues in which the cysteinyl moiety of ACV is replaced with serine or cysteic acid fail to elicit the characteristic EPR and optical features despite the fact that they are bound with reasonable affinity to the enzyme. These results demonstrate that the thiolate of ACV coordinates the Fe^{2+}. The EPR spectra of both the IPNS·NO and IPNS·ACV·NO complexes are broadened for samples prepared in ^{17}O-enriched water, showing that water (or hydroxide) is also an iron ligand in each case. Thus, the Fe^{2+} coordination of the IPNS·ACV·NO complex accommodates at least three exogenous ligands. Photodissociation of NO from this complex results in a species exhibiting nearly the same Mössbauer spectrum as the IPNS·ACV complex, suggesting that NO addition does not result in a major change in other aspects of the Fe^{2+} coordination.

Isopenicillin N synthase (IPNS)[1] catalyzes the stereospecific formation of the β-lactam and thiazolidine rings of isopenicillin N from the linear tripeptide ACV[1] as indicated in Scheme I (Pang et al., 1984; Baldwin & Abraham, 1988).

Although O_2 is required for the reaction, no oxygen is incorporated into the product, suggesting the oxidase chemistry illustrated (White et al., 1982; Ingraham & Meyer, 1985). The active site of IPNS contains a catalytically essential Fe^{2+} (Chen et al., 1989) that might be expected to catalyze this chemistry. However, no iron-bound oxygen intermediate has yet been detected, leaving the role of the metal in catalysis undefined. Nevertheless, a direct role for iron has been proposed on the basis of extensive studies by Baldwin and coworkers [as reviewed by Baldwin and Abraham (1988) and Baldwin and Bradley (1990)], which showed that oxygen is incorporated during turnover of some ACV analogues. This result is consistent with metal-catalyzed oxygenase chemistry

† This work was supported in part by Grants GM-24689 (to J.D.L.) and GM-22701 (to E.M.) from the National Institute of General Medical Science.

* Correspondence can be addressed to either of these authors. The address for V.J.C. is Lilly Research Laboratories, MC797, Lilly Corporate Center, Indianapolis, IN 46285.

‡ University of Minnesota.

§ Lilly Research Laboratories.

∥ Present address: Biology Division, Oak Ridge National Laboratory, Oak Ridge, TN 37831.

⊥ Carnegie Mellon University.

[1] Abbreviations: ACV, (L-α-amino-δ-adipoyl)-L-cysteinyl-D-valine; ASV, (L-α-amino-δ-adipoyl)-L-serinyl-D-valine; $AC(SO_3^-)V$, (L-α-amino-δ-adipoyl)-L-cysteyl-D-valine; ACA(Cl), (L-α-amino-δ-adipoyl)-L-cysteinyl-β-chloro-D-alanine; ACG, (L-α-amino-δ-adipoyl)-L-cysteinylglycine; Ph(3-COOH)AcCV, (3-carboxyphenyl)acetyl-L-cysteinyl-D-valine; Cys-255→Ser, site-specific mutant in which Cys-255 is changed to serine; Cys-106→Ser, site-specific mutant in which Cys-106 is changed to serine; Cys-106,255→Ser, site-specific mutant in which Cys-255 and Cys-106 are both changed to serine; IPNS, isopenicillin N synthase; EDTA, ethylenediaminetetraacetic acid; DTT, 1,4-dithiothreitol; MOPS, 3-(*N*-morpholino)propanesulfonic acid; EXAFS, extended X-ray absorption fine structure; ESEEM, electron spin echo envelope modulation.

0006-2960/92/0431-4602$03.00/0

Scheme I[a]

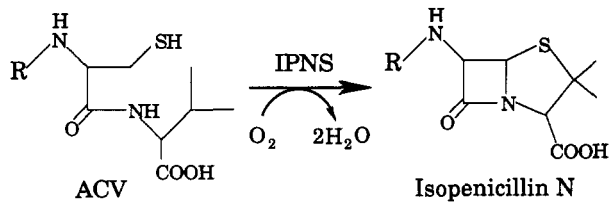

[a] R = L-α-amino-δ-adipoyl.

that would be facilitated by coordination of the electron-donating thiolate moiety of the substrate. Consequently, the current mechanistic proposals adopt both Fe·ACV and Fe·O_2 bonds at various stages of the catalytic cycle (Baldwin & Abraham, 1988; Baldwin & Bradley, 1990). More direct evidence for an Fe·ACV thiolate bond has recently been derived from spectroscopic studies (Chen et al., 1989; Ming et al., 1990, 1991; Jiang et al., 1991). In the first of these studies, Mössbauer spectra of ^{57}Fe-enriched IPNS showed that the iron ligation becomes much more covalent upon formation of the ACV complex (Chen et al., 1989), resulting in a decrease in the value of the isomer shift parameter. The decrease observed was approximately that expected from comparisons of Mössbauer spectra of other well-studied iron–thiolate complexes with those of analogous complexes devoid of thiolate. Moreover, the optical spectrum of the IPNS·NO complex was shown to change from pale yellow to pink (λ_{max} = 508 nm) upon complexation of ACV, consistent with the formation of a thiolate-to-metal charge-transfer complex between the ACV thiolate and the iron. Similarly, an intense electronic absorption was observed when ACV associated with IPNS in which Fe^{2+} had been replaced by Cu^{2+}, consistent with a thiolate-to-Cu^{2+} charge-transfer transition (Ming et al., 1990). Additional evidence for ACV–thiolate ligation of the iron is presented in the accompanying EXAFS study (Scott et al., 1992), in which it is shown that the difference between the spectra of IPNS and the IPNS·ACV complex can be accounted for by the inclusion of one sulfur in the iron coordination sphere.

Despite the substantial evidence for introduction of the ACV thiolate into the iron coordination, the data available cannot be used to rule out the case in which a conformational change coincident with ACV binding results in the binding of a protein-derived cysteinyl thiolate to the iron. Indeed, in all of the well-studied IPNS enzymes isolated from fungi and bacteria, two cysteines are conserved, suggesting that these residues play essential roles (Pang et al., 1984; Samson et al., 1985; Carr et al., 1986; Ramon et al., 1987; Weigel et al., 1988; Leskiw et al., 1988; Shiffman et al., 1988; Castro et al., 1988; Palissa et al., 1989). The 38.4-kDa enzyme isolated from *Cephalosporium acremonium* contains only two cysteines, located at positions 106 and 255 (Samson et al., 1985; Miller & Ingolia, 1989). They are present as free thiols in the apoenzyme (Kriauciunas et al., 1991). The functional role and accessibility of the cysteines have been probed by various chemical approaches, leading in some cases to different conclusions. For example, Baldwin et al. (1990) showed that Cys-255, but not Cys-106, is modified by a photoactivated diazirinyl analogue of ACV, whereas Kriauciunas et al. (1991) have found that Cys-106 and not Cys-255 reacts with *N*-ethylmaleimide. In another approach, site-specific mutagenesis has been used to evaluate the role of the cysteines (Samson et al., 1987; Kriauciunas et al., 1991). These studies indicated that the mutation of Cys-106 to Ser resulted in substantially decreased catalytic efficiency. However, mutation of the cysteines either individually or in concert failed to completely eliminate catalytic activity, showing that the cysteines are not essential for the reaction chemistry. Consequently, the precise roles of the cysteines in catalysis, and their possible role as iron ligands at some stage of the reaction cycle, remain to be elucidated.

In the current study, the active site ligation of the IPNS substrate complex is addressed by three approaches. In the first approach, the Mössbauer, EPR, and optical spectra of the Cys → Ser mutant enzymes and their complexes with ACV and NO (an O_2 analogue) are compared with those of the wild-type enzyme to assess the role of the endogenous cysteines as potential iron ligands. In the second approach, the role of the thiolate moiety of ACV as an iron ligand is assessed through the use of ACV analogues in which the thiol or other portions of the substrate molecule are altered. Finally, the ability of water to coordinate at the same time as NO or NO *and* ACV to the active site Fe^{2+} is assessed through the use of EPR-detected nuclear hyperfine interactions from ^{17}O-enriched water in the enzyme–nitrosyl complexes. The data support an active site iron which is simultaneously coordinated by the thiolate moiety of ACV, water, and NO in the ternary nitrosyl complex, implying direct participation of the iron in catalysis.

Experimental Procedures

Chemicals. Water enriched to ~50 atom % in ^{17}O was obtained from Icon Services Inc. The enriched water was neutralized, treated with activated charcoal, and distilled twice in a microdistillation apparatus before use. Nitric oxide was supplied by Matheson and used after passage through a bed of solid NaOH pellets. ^{57}Fe enriched to 95 atom % was obtained from Icon Services, Inc., and prepared for use as previously described (Chen et al., 1989). ACV was obtained from Incell. A large fraction of the ACV was found to be present as disulfide dimers when dissolved in the solutions used in this study. Consequently, an equal amount of DTT was added with the ACV. Control experiments showed that DTT up to 100 mM added to the enzyme without ACV had no effect on the Mössbauer, EPR, or optical spectra and did not inhibit the reaction. Control EPR and optical experiments were also conducted without DTT added to the ACV, and equivalent results were obtained. The ACV analogues ACG, ASV, and Ph(3-COOH)AcCV were provided by R. B. Rothenberger and P. D. Gesellchen of Lilly Research Laboratories, and ACA(Cl) was provided by J. J. Osborne and P. D. Gesellchen of Lilly Research Laboratories. AC(SO_3^-)V was prepared by performate oxidation of ACV according to the established procedures (Hirs, 1967). All other chemicals were reagent grade and used without further purification. Unenriched water was deionized and then glass distilled.

Enzyme Expression, Purification, and Assays. The cloning of IPNS, site-specific mutation procedures, and expression of recombinant enzymes have been previously described (Samson et al., 1985; Baldwin et al., 1987; Kriauciunas et al., 1991). The recombinant enzyme, referred to as "wild-type" in this study, exhibited specific activities of 7–9 units/mg. This specific activity is greater than that originally reported for enzyme isolated directly from *C. acremonium* (Pang et al., 1984), but comparable to that which we have observed for recent preparations of the natural enzyme (Kriauciunas et al., 1991). IPNS oxidase activity was routinely assayed by measuring the oxygen uptake with a Clark-type oxygen electrode as previously described (Chen et al., 1989). Typical assays were carried out at 25 °C in air-saturated MOPS buffer at pH 7.1 containing 5 mM ascorbate and 5 mM ACV. The mutant enzymes exhibited the same catalytic properties as

previously described (Kriauciunas et al., 1991).

Anaerobic Procedures and Nitric Oxide Addition. Samples were made anaerobic by repeated cycles of evacuation and flushing with argon that had been passed over a column of BASF Inc. copper catalyst at 170 °C to remove residual oxygen. For parallel optical and EPR studies, anaerobic enzyme, substrate, and inhibitor solutions were prepared separately in serum-stoppered vials. The enzyme and, where indicated, the substrate or inhibitor were then transferred with gas-tight syringes into an anaerobic optical cuvette under positive Ar pressure. Nitric oxide [either 100% NO or 2% NO diluted with He (Matheson)] was added by displacing the Ar in the head space. An incubation of approximately 10 min while mixing gently at 5 °C was required to saturate the sample. A sample was then removed from the optical cuvette with a gas-tight syringe, transferred to an anaerobic serum-stoppered EPR tube, and then frozen by slow immersion in liquid nitrogen. Use of the 2% NO concentration was generally sufficient to elicit the maximal EPR signal and enzyme-associated optical spectra. Identical results were obtained regardless of the order of addition of ACV and NO. Nitric oxide is highly toxic, requiring that all additions and transfers be conducted in a ventilated hood.

Sample Preparation in ^{17}O-Enriched Water. EPR samples containing ^{17}O-enriched water were made by adding ^{17}O-enriched water to IPNS previously lyophilized in 100 mM MOPS buffer at pH 7.1. Control samples were prepared in the same manner using unenriched water. Both unenriched and ^{17}O-enriched water were adjusted to pH 7.1 immediately before enzyme rehydration by addition of small volumes of 2 M MOPS at pH 7.1. Sample concentrations were determined by measuring the optical densities at 280 nm. Substrate was added from a concentrated solution prepared in unenriched water and represented only a 1% dilution of the original sample. The rehydrated enzyme showed the same high specific activity as the enzyme before lyophilization.

Spectroscopy. Optical spectra were recorded using a Hewlett Packard 8451A diode array spectrophotometer at 10 °C. EPR spectra were recorded at X-band with a Varian E-109 spectrometer equipped with an Oxford Instruments ESR-910 liquid helium cryostat. Temperature and g-value calibrations were as previously described (Lipscomb, 1980). Data were recorded for integration and subtraction procedures with a digital computer interfaced directly to the spectrometer. Spin quantitations were performed by double integration of the first derivative spectra by the method of Aasa and Vänngård (1975). Mössbauer samples were prepared and the spectra recorded and analyzed as previously described (Chen et al., 1989). Isomer shifts are quoted relative to iron metal at room temperature. EPR and Mössbauer spectra of spin $S = {}^3/_2$ complexes were analyzed as previously described (Arciero et al., 1983). It is convenient to differentiate between $S = {}^3/_2$ spectra on the basis of E/D, where E and D are parameters from the spin Hamiltonian formulation. The term E/D is a measure of the deviation of the electronic environment of the iron from axial symmetry that can assume values between 0 and ${}^1/_3$ (Blumberg, 1967; Blumberg & Peisach, 1973), the extreme values representing the axial and completely rhombic cases, respectively. If g_0 is assumed to be equal to 2, the absolute value of E/D can be calculated from the g-values.

Photodissociation Procedures. EPR samples were irradiated with light from a 300-W quartz halogen lamp through the metal grid of the EPR cavity while the sample temperature was maintained near 5 K. IR energy was removed using either an IR filter, IR mirror, or a band-pass filter (Oriel Inc.). The band-pass filters were used to supply light of specific wavelengths (±10 nm). The power of white light incident on the cavity grid was adjusted to 42 mW as measured using a Spectra-Physics Model 404 radiant power meter. The incident power of light after passage through the band-pass filters was adjusted to 0.4 mW. Heating of the sample due to the irradiation was estimated by monitoring the loss of EPR signal amplitude of a sample of protocatechuate 3,4-dioxygenase [prepared as described by Whittaker et al. (1984, 1990)] with the same optical density at 430 nm as the IPNS samples. The incident white light caused about 1-deg increase in temperature at 4.2 K while the band-pass-filtered light caused no detectable increase. The rate of photodissociation was monitored as loss of the EPR signal at $g = 4.22$ and fit to a one- or two-exponential time course using nonlinear regression (Whittaker & Lipscomb, 1984). The rate of dissociation was not appreciably affected by inclusion of 50% v/v glycerol in the sample to create a glass.

Photodissociation of Mössbauer samples was performed using white light from a 500-W projector lamp directed through a 1-m quartz light pipe into the sample mounted in the instrument Dewar. A specially designed Lucite Mössbauer cup was utilized that contained a center post to allow light to penetrate to the center of the sample. The glassed sample was maintained at 4.2 K and was exposed to white light for 30 min prior to starting the data collection. The sample was reirradiated for 30 min at approximately 12-h intervals. Following the completion of the experiment, the sample was warmed to 77 K for 10 min to allow rebinding of the NO. Complete rebinding was demonstrated by measuring the 4.2 K Mössbauer spectrum.

Table I: Mössbauer Parameters of Wild-Type and Cys-106,255→Ser Isopenicillin N Synthase[a]

		ligand		
			+35 mM ACV	
enzyme	parameters	none	species I	species II
wild type	ΔE_Q (mm/s)	2.70	2.69	3.43
	δ (mm/s)	1.30	1.30	1.11
	fraction	1.00	0.35	0.65
Cys-106,255→Ser	ΔE_Q (mm/s)	2.79	2.81	3.37
	δ (mm/s)	1.29	1.29	1.10
	fraction	1.00	0.75	0.25

[a] Experimental conditions are described in Figure 1.

Results

Studies with Mutant Enzymes. (A) Mössbauer Spectroscopy of Cys-106,255→Ser Mutant IPNS. The apo-IPNS spontaneously takes up 1 mol of Fe^{2+}/mol of protein to reconstitute fully active holoenzyme (Chen et al., 1989). Stoichiometric iron uptake was also observed for each of the Cys → Ser mutant proteins, even though the specific activity and steady-state kinetic parameters of these enzymes differed from those of the wild-type enzyme (Kriauciunas et al., 1991). The 4.2 K Mössbauer spectra of the $^{57}Fe^{2+}$-reconstituted wild-type (Figure 1A) and Cys-106,255→Ser mutant IPNS (Figure 1B) consist of single quadrupole doublets with nearly identical parameters (Table I) characteristic of high-spin Fe^{2+}. Therefore, replacement of all the protein-derived cysteines does not significantly alter the Fe^{2+} ligand environment.

Anaerobic addition of 35 mM ACV to the wild-type and Cys-106,255→Ser IPNS resulted in the Mössbauer spectra shown in parts C and D, respectively, of Figure 1. Each spectrum consists of two quadrupole doublets, one of which

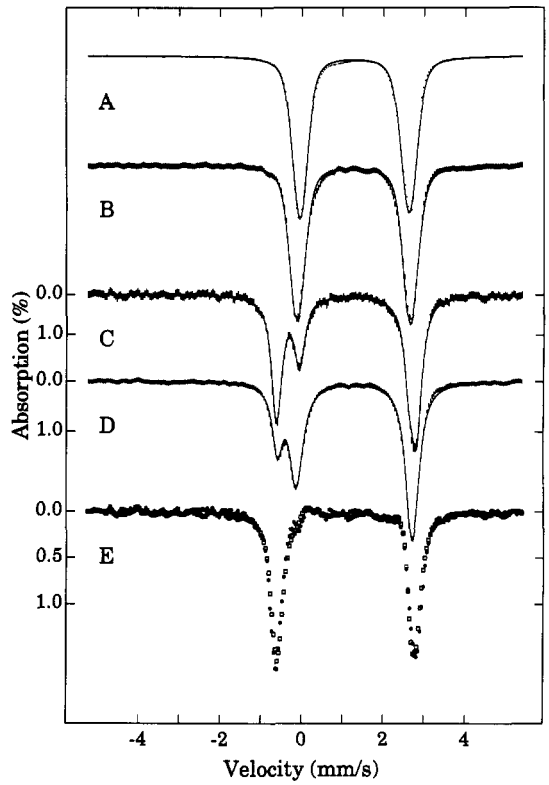

FIGURE 1: Mössbauer spectra of Fe(II) IPNS and Fe(II) IPNS·ACV. (A) 4.5 mM $^{57}Fe^{2+}$-reconstituted wild-type enzyme and (B) 2.5 mM $^{57}Fe^{2+}$-reconstituted Cys-106,255→Ser mutant enzyme in 50 mM MOPS buffer, pH 7.1; (C) 1.8 mM wild-type IPNS and (D) 2.0 mM Cys-106,255→Ser IPNS after anaerobic addition of 35 mM ACV. The spectra of (A) and (B) have non-Lorentzian lines which can be reasonably well described by a Voigt profile with 0.25 mm/s Lorentzian width and 0.38 mm/s Gaussian width. The solid lines shown in (C) and (D) are least squares fits based on the parameters shown in Table I. (E) Normalized spectra of the wild-type (●) and doubly-mutated (□) IPNS·ACV complexes obtained after subtracting the Fe(II) IPNS spectra from (C) and (D). The spectra of (B) and (D) were recorded with a larger velocity sweep and then scaled to the sweep employed for spectra of (A) and (C). All spectra were obtained at 4.2 K in a 60-mT magnetic field applied parallel to the direction of the observed γ-rays.

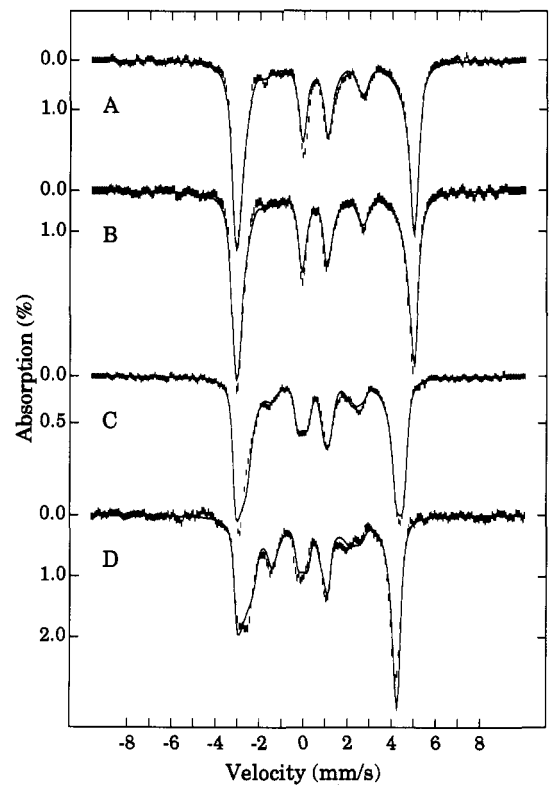

FIGURE 2: 4.2 K Mössbauer spectra of the nitrosyl complexes of Fe(II) IPNS and Fe(II) IPNS·ACV. Each sample was made anaerobic and stirred under 100% NO gas at 5 °C as described in Experimental Procedures. Spectra A–C were obtained at 4.2 K in 60-mT magnetic field applied parallel to the direction of the observed γ-rays. (A) 1.3 mM wild-type and (B) 2.4 mM Cys-106,255→Ser mutated IPNS in anaerobic 50 mM MOPS buffer, pH 7.1; (C) sample from (B) plus 35 mM ACV; (D) sample from (C) in 6.0-T applied field. The solid lines are computer simulations based on the spin Hamiltonian of eq 3 using the parameters of Table II. A quadrupole doublet of a diamagnetic species corresponding to 4% and 5% of spectra A and C, respectively, was subtracted from the data prior to computer simulations (see footnote 3).

is due to the ACV-bound complex, while the other is due to uncomplexed enzyme. Figure 1E demonstrates the near identity of the spectra of the enzyme·ACV complexes. As we have argued previously (Chen et al., 1989), the significantly decreased value of the isomer shift associated with the enzyme·ACV complex (≈0.2 mm/s) indicates a more covalent iron ligand environment, consistent with the addition of a thiolate ligand to the iron in both the wild-type and doubly-mutated enzymes. The only source of this thiolate in the doubly-mutated enzyme is the cysteinyl moiety of ACV.[2]

The fits to the data shown in Figure 1C,D (solid lines) indicate that the Cys-106,255→Ser IPNS forms less of the ACV complex than the wild-type enzyme (wild type, 65%; mutant, 25%) (Table I). This implies a change in the binding affinities for ACV; K_D values for the ACV complex of ~18 mM and ~105 mM were calculated for the wild-type and mutant enzymes, respectively. This result is in accord with the steady-state turnover kinetics, which showed that the double mutant has a 14-fold higher K_M value for ACV than for the wild-type enzyme (Kriauciunas et al., 1991).

Both the wild-type and Cys-106,255→Ser IPNS enzymes bind nitric oxide to produce species with electronic spin, $S = {}^3/_2$ (Chen et al., 1989). The Mössbauer spectra of these complexes taken in parallel applied magnetic field of 0.06 T are shown as spectra A and B, respectively, in Figure 2. Within experimental uncertainty, these spectra are identical.[3] When ACV binds to the enzyme–nitrosyl complex, the electronic spin remains $S = {}^3/_2$ but the rhombicity of the complex changes, resulting in markedly different Mössbauer and EPR spectra. Spectra C and D of Figure 2 show 4.2 K Mössbauer spectra of the Cys-106,255→Ser IPNS·ACV·NO complex taken in parallel applied magnetic fields of 0.06 and 6 T, respectively. Identical spectra were obtained for wild-type IPNS·ACV·NO (see Figure 6A).

[2] Coordination of sulfur from methionine cannot be explicitly ruled out by the data reported here. However, to the best of our knowledge, in no instance has a methioninyl sulfur–iron ligation resulted in a charge-transfer transition of the type observed (see optical results).

[3] Upon prolonged incubation of IPNS in the presence of NO, a new species consisting of a quadrupole doublet with $\Delta E_Q = 1.01$ mm/s and $\delta = 0.16$ mm/s is observed in 100% yield. In samples incubated for shorter time periods, this species is formed in lesser amounts (typically 3–5% of the total iron). Detailed characterization of this species has not been attempted. However, the Mössbauer parameters are consistent with the assignment to an $S = 0$ species. The addition of ACV does not perturb the Mössbauer spectrum of this species. Upon detailed analysis, some of the $S = {}^3/_2$ nitrosyl complexes of IPNS were observed to contain small fractions of this species. For the spectra presented here, the contribution of this species has been subtracted from the experimental data before computer simulations were performed.

Table II: Mössbauer Parameters of $S = {}^3/_2$ Nitrosyl Complexes of Wild-Type and Cys-106,255→Ser Mutant Isopenicillin N Synthase[a]

parameter	IPNS·NO	IPNS·ACV·NO	Fe(II)·EDTA·NO
D (cm^{-1})	14 (1)[b]	14 (1)	12 (1)
E/D	0.015 (1)	0.035 (1)	0.020 (1)
ΔE_Q (mm/s)	−1.0 (1)	−1.2 (1)	−1.72 (3)
η	0.1 (2)	1.0 (2)	0
A_x (MHz)	−35 (1)	−31 (1)	−32 (1)
A_y (MHz)	−33 (1)	−28 (1)	−32 (1)
A_z (MHz)	−45 (4)	−34 (3)	−43 (4)
δ (mm/s)	0.75 (3)	0.65 (3)	0.66 (3)
α, β, γ[c] (deg)	0, 8, 0	10, 20, 0	0, 10, 0

[a] The spectra of the wild-type and mutant enzyme complexes were best fit with the same sets of parameters. The preparation of the enzyme–nitrosyl complexes is described in Experimental Procedures. The nitrosyl complex of reduced iron–EDTA complex was that prepared by Arciero et al. (1983). [b] Numbers in parentheses give the uncertainty in the least significant digit. [c] α, β, and γ are the Euler angles that simultaneously rotate the **A** and electric field tensors relative to the zero-field splitting tensor.

The solid lines in Figure 2 are computer fits to the spectra performed within the framework of the $S = {}^3/_2$ spin Hamiltonian:

$$\mathbf{H} = \mathbf{H}_e + \mathbf{H}_n \quad (1)$$

$$\mathbf{H}_e = g_0\beta_e\vec{H}\cdot\vec{S} + D[S_z^2 - (1/3)S(S+1) + (E/D)(S_x^2 - S_y^2)] \quad (2)$$

$$\mathbf{H}_n = \vec{S}\cdot\tilde{\mathbf{A}}\cdot\vec{I} + (eQV_{zz}/12)[3I_z^2 - I(I+1) + \eta(I_x^2 - I_y^2)] - g_n\beta_n\vec{H}\cdot\vec{I} \quad (3)$$

where all symbols have their conventional meanings. The values of $g_0 = 2$ and $E/D = 0.015$ for IPNS·NO and $E/D = 0.035$ for IPNS·ACV·NO were obtained from the EPR spectra (see below). Both Mössbauer and EPR spectroscopies show that $D > 0$ (data not shown). The properties of the $m_s = \pm{}^1/_2$ ground Kramers doublet are such that the Mössbauer ^{57}Fe nucleus samples preferentially the parameters in the x–y plane of the electronic system. Thus, the spectrum of Figure 2C depends principally on A_x, A_y, and the components of the electric field gradient tensor in the x–y plane (V_{xx} and V_{yy}). From fits to these spectra and the corresponding spectra taken in transverse field, A_x, A_y, ΔE_Q, and η [where $\Delta E_Q = (eQV_{zz}/2)[1 + (1/3)\eta^2]^{1/2}$] were obtained. In a field of 6.0 T, the applied field mixes the $m_s = \pm{}^3/_2$ doublet into the ground doublet. This mixing depends on the energy separation $\Delta \approx 2D$ of the two doublets. By matching the magnetic splittings observed for $H = 0.06$ T and $H = 6$ T, D was determined to be 14 ± 1 cm^{-1}. Owing to the axial nature of the electronic system, the Mössbauer spectra are relatively insensitive to the z-component of the magnetic hyperfine tensor, A_z. However, by fitting the entire data set, including the spectra taken in transverse field, the value of A_z could be determined with reasonable accuracy. Our analysis shows clearly that the magnetic hyperfine interactions of the IPNS nitrosyl complexes have considerable anisotropies. In our earlier analysis of the Fe(II)·EDTA·NO complex (Arciero et al., 1983), we had assumed that the **A**-tensor was isotropic. These data have been reexamined in the context of the current study with the conclusion that $\tilde{\mathbf{A}}$ is anisotropic for Fe(II)·EDTA·NO as well. The parameter sets used to fit the spectra of IPNS·ACV·NO and IPNS·NO, as well as the newly determined parameters for Fe(II)·EDTA·NO, are collected in Table II.

Comparison of the parameter sets of IPNS·NO and IPNS·ACV·NO reveals that the magnetic hyperfine interactions of IPNS·ACV·NO are about 15% smaller than those obtained for IPNS·NO. Similarly, the isomer shift is noticeably smaller for the IPNS·ACV·NO complex. Both observations are in accord with the notion that the thiolate of ACV is coordinated to the metal; similar trends in $\tilde{\mathbf{A}}$ and δ are, for instance, observed when cytochrome P450 (iron–thiolate) and myoglobin (iron–histidyl) are compared.[4] It is noteworthy that the zero-field splitting is the same for both IPNS·NO and IPNS·ACV·NO. Finally, the analysis presented here shows clearly that the magnetic hyperfine tensors of both complexes exhibit considerable anisotropy. This information will need to be taken into account when various bonding descriptions for these unusual iron–nitrosyl complexes are considered.[5]

Table III: Spectroscopic Parameters of the Nitrosyl Complexes of Wild-Type and Site-Specific Mutant IPNS Enzymes[a]

		technique		
			optical	
enzyme	additions	EPR (E/D)	λ_{max} (nm)	ϵ (cm^{-1} M^{-1})
wild type	+NO	0.015	430	800
	+ACV + NO	0.035	508	1850
Cys-255→Ser	+NO	0.015	430	850
	+ACV + NO	0.035	508	1750
Cys-106→Ser	+NO	0.015	440	700
	+ACV + NO	0.035	508	1800
Cys-106,255→Ser	+NO	0.015	438	900
	+ACV + NO	0.035	508	2300

[a] Experimental conditions are described in Figures 3 and 4.

The spectra of both the wild-type (see Figure 6A) and double mutant (Figure 2C,D) IPNS·ACV·NO complexes consist of single species (see footnote 3), showing that the enzyme is saturated with both NO and ACV. This is markedly different from the IPNS·ACV complex, which exhibits only partial binding of ACV at the same substrate concentration (see, for example, Figure 1C,D). Thus, ACV apparently binds much more tightly to the enzyme after NO is bound. The fact that this coupling of exogenous ligand binding is observed for the double mutant IPNS shows that the increase in ACV affinity engendered by NO binding is sufficient to overcome the inherently decreased affinity for substrate of the mutant enzymes.

(B) EPR Spectroscopy of the Cys-106→Ser, Cys-255→Ser, and Cys-106,255→Ser Mutant IPNS Nitrosyl Complexes. Complementary information about the paramagnetic species observed in the Mössbauer spectra of the nitrosyl complexes can be obtained from EPR spectroscopy.[6] Addition of NO to each of the three $^{56}Fe^{2+}$-reconstituted mutant IPNS enzymes resulted in species exhibiting essentially identical $S = {}^3/_2$ EPR

[4] The isomer shifts at 4.2 K of ferrous cytochrome P450 and deoxymyoglobin are $\delta = 0.84$ mm/s (Sharrock et al., 1973) and $\delta = 0.96$ mm/s (Kent et al., 1983), respectively; the magnetic hyperfine interactions for both proteins are not well enough analyzed for useful comparisons. However, the magnetic hyperfine coupling constant of high-spin ferric cytochrome P450 (Sharrock et al., 1973; Champion et al., 1975) is 11% smaller than that of metmyoglobin (Lang, 1970; Scholes et al., 1973).

[5] For instance, a scheme with antiferromagnetic coupling between a high-spin ferric ($S_1 = {}^5/_2$) ion and an $S = 1$ NO^- moiety would have to allow for considerable anisotropic covalency in order to explain the observed **A**-tensor anisotropies.

[6] The EPR spectra of the Mössbauer samples were identical to those observed for samples not enriched with ^{57}Fe except for line width. Hyperfine broadening of 1.46 mT was observed in the $g = 1.99$ resonance of the ^{57}Fe-enriched IPNS·NO complex. Broadenings of 0.25, 0.4, and 1.1 mT were observed for the $g = 4.22$, 3.88, and 1.98 resonances, respectively, of the ^{57}Fe-enriched IPNS·ACV·NO complex.

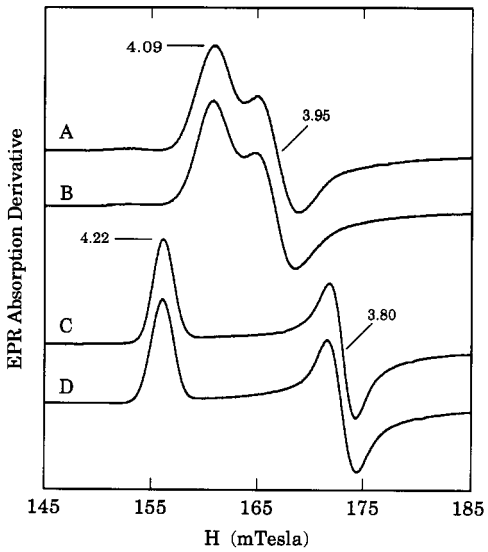

FIGURE 3: EPR spectra of wild-type and Cys-106,255→Ser IPNS·NO complexes. All samples contained 300 μM enzyme in 100 mM MOPS buffer at pH 7.1. Nitrosyl complexes of all samples were formed by exposure to 2% NO to give ~67 μM free NO in solution at equilibrium. (A) Wild-type IPNS; (B) Cys-106,255→Ser IPNS; (C) wild-type IPNS plus 1.5 mM ACV; (D) Cys-106,255→Ser IPNS plus 100 mM ACV. EPR spectra equivalent to that shown in (D) were obtained from the sample used to collect the Mössbauer data shown in Figure 2C. Instrumental conditions: microwave power = 0.2 mW; microwave frequency = 9.22 GHz, temperature = 5 K; modulation frequency = 100 kHz; modulation amplitude = 1 mT.

spectra (Table III). The spectra of the wild-type and Cys-106,255→Ser enzymes are compared in parts A and B, respectively, of Figure 3. Each enzyme exhibited a single species with an E/D of 0.015. The species was fully formed in each case when the dissolved (uncomplexed) NO concentration was ~67 μM, showing that the K_D values for the nitrosyl complexes are significantly lower than this value. A comparable value was reported previously for the wild-type enzyme (Chen et al., 1989).

The IPNS·NO·ACV complexes of the wild-type and the mutant enzymes exhibited indistinguishable $S = {}^3/_2$ EPR spectra with an $E/D = 0.035$ (Table III, Figure 3C,D). In each case, only a single species is present, accounting for greater than 90% of the iron present in the sample. These results show that the substrate complex is completely formed at only 1.5 mM ACV, again demonstrating that the NO greatly increases the affinity of the enzyme for ACV (compare with Figure 1C).

(C) Optical Spectra of the Cys-106→Ser, Cys-255→Ser, and Cys-106,255→Ser IPNS Nitrosyl Complexes. Figure 4A compares the optical spectra of the Cys-106,255→Ser IPNS·NO complex (solid line) with the wild-type IPNS·NO complex (dashed line). The spectra are very similar, each exhibiting a broad maximum at 430 nm and a weak band at about 630 nm. The optical spectra of each of the single Cys → Ser mutants are also very similar to that shown in Figure 4A (Table III). Figure 4B compares the optical spectra obtained after anaerobic addition of ACV to the samples of Figure 4A. Again, these spectra, as well as those observed for the other two Cys → Ser mutant enzymes, are very similar. The large increases in molar absorptivity and the visible absorbance band at 508 nm are consistent with thiolate ligation to the iron in each case. The complete formation of the 508-nm chromophore correlates with addition of a nearly stoichiometric concentration of ACV, consistent with the large increase in enzyme affinity for ACV engendered by NO described above (data not shown).

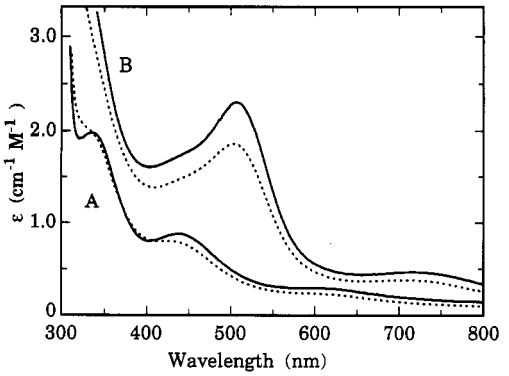

FIGURE 4: Optical spectra of Cys-106,255→Ser IPNS·NO complexes. All samples were prepared and NO added as described in Figure 3 and Experimental Procedures. (A) Wild-type (---) and Cys-106,255→Ser (—) enzyme; (B) samples from (A) after addition of 1.5 mM ACV to the wild-type (---) or 100 mM ACV to the Cys-106,255→Ser (—) enzyme.

(D) Photodissociation of the IPNS·ACV·NO Complex. Photodissociation of heme–nitrosyl complexes has been extensively studied and has provided valuable insight into the structural changes in the heme site caused by small ligand binding (Yoshida et al., 1980; Boelens et al., 1982). We have observed analogous photodissociation of NO from nonheme Fe^{2+} centers of catecholic dioxygenases (Lipscomb & Orville, 1992). As shown in Figure 5, inset, exposure of the IPNS·ACV·NO complex to intense light at 2–10 K results in a decrease of the EPR signal from the $S = {}^3/_2$ species at a rate dependent on both the intensity and the wavelength of the illumination source, indicating that the NO is photodissociated. After the light is switched off, the $S = {}^3/_2$ signal reappears with a half-life in excess of 15 h at 5 K. The $S = {}^3/_2$ signal intensity observed at 5 K is fully restored by warming the sample to 77 K for a few seconds, showing that NO reassociates with the active site iron in the frozen matrix. Figure 5 shows the time course for the photodissociation time course for white light (A) and light of 510 nm (B) and 720 nm (C). At least two summed exponentials were required to fit the photodissociation time course at 510 nm, indicating that the process is complex. This is not atypical of small-molecule photodissociation and reassociation processes (Boelens et al., 1982; Austin et al., 1975). Nitric oxide was most efficiently dissociated by light in the visible absorption band (410–560 nm); however, the wavelength dependence of the quantum efficiency must be determined for this type of metal center before more precise correlations can be made between the observed visible transitions and photodissociation (Boelens et al., 1982). The NO was also observed to be photodissociated from the IPNS·NO complex by light at 430 nm (not shown). However, only partial dissociation was observed even on exposure to white light.

Figure 6 shows the 4.2 K Mössbauer spectra of the IPNS·ACV·NO complex before and after photodissociation of NO at 4.2 K. Upon exposure to white light, the $S = {}^3/_2$ complex (Figure 6A) is converted to a high-spin ferrous species with $\Delta E_Q = 3.27$ mm/s and $\delta = 1.09$ mm/s (Figure 6B). After warming the sample briefly to 77 K, the 4.2 K Mössbauer spectrum was restored to that shown in Figure 6A, demonstrating that the photodissociation of NO is a reversible process. Within the experimental accuracy, the isomer shift of the photodissociated complex is the same as that observed for IPNS·ACV formed by equilibrium binding at room temperature before freezing, while ΔE_Q is about 4% smaller. After photodissociation, the NO binding site is expected to remain unoccupied at 4.2 K. The similarity of the Mössbauer pa-

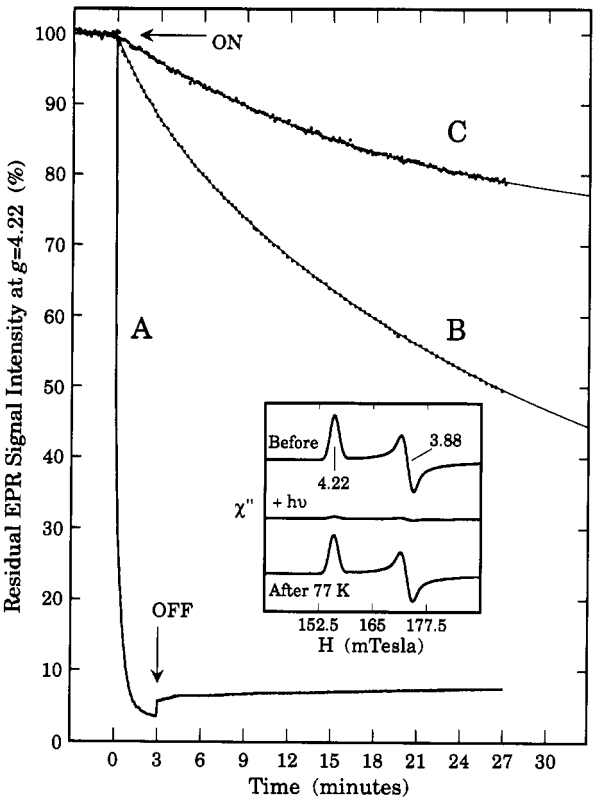

FIGURE 5: Kinetics of photodissociation of the IPNS·ACV·NO complex at 5 K. IPNS (1.1 mM) in anaerobic 100 mM MOPS, pH 7.1, plus 50% glycerol was mixed with 11 mM ACV and exposed to NO (100%) before freezing. The $g = 4.22$ resonance was monitored at a constant field (155.8 mT), and all other instrumental conditions were as in Figure 3. Photolysis at 5 K was initiated by removing an opaque shutter at the time marked by the arrow. Photolysis induced by (A) white light (350–800 nm), (B) light at 510 ± 10 nm, (C) light at 720 ± 10 nm. Decay traces B and C were measured at the same power. The solid line in (B) is a fit to two summed exponential decays ($k_1 = 5.05 \times 10^{-3}$ s^{-1}; $k_2 = 5.41 \times 10^{-4}$ s^{-1}). The solid line in (C) is a fit to one exponential decay ($k = 8.18 \times 10^{-4}$ s^{-1}). At higher power, the dissociation at 720 nm was also found to be best fit by two summed exponentials. In trace A, the opaque shutter was replaced at the time indicated by the arrow. Inset: EPR spectra of the $g = 4$ region of the sample from the main figure. Top: Before illumination. Middle: After illumination with white light. Bottom: After warming the sample to 77 K for 5 min and then cooling to 5 K.

rameters raises the question of whether the NO binding site is also unoccupied in the IPNS·ACV complex formed at room temperature. Without some knowledge of the ligand field parameters, we presently do not know the sensitivity of ΔE_Q to changes in the coordination sphere of this iron site (the desired information may be obtained from high-field Mössbauer or MCD studies). Thus, it is conceivable the small change in ΔE_Q is due to the presence of an easily displaced ligand such as water in the NO binding site at room temperature. Alternatively, the site may be unoccupied at room temperature and the difference in ΔE_Q may reflect an inability of the ligand sphere to relax at 4.2 K to its equilibrium structure; such trapped conformational states have been observed in the photodissociation of myoglobin (Austin et al., 1975). Whatever the reason for the small difference in ΔE_Q, it seems unlikely that major changes occur in the coordination sphere of IPNS·ACV upon NO binding and photodissociation. Mössbauer spectra of photodissociated IPNS·NO complex could not be obtained due to the relatively low photodissociation efficiency.

Studies Using ACV Analogues. EPR and Optical Spectra of Nitrosyl Complexes of Wild-Type IPNS with Substrate

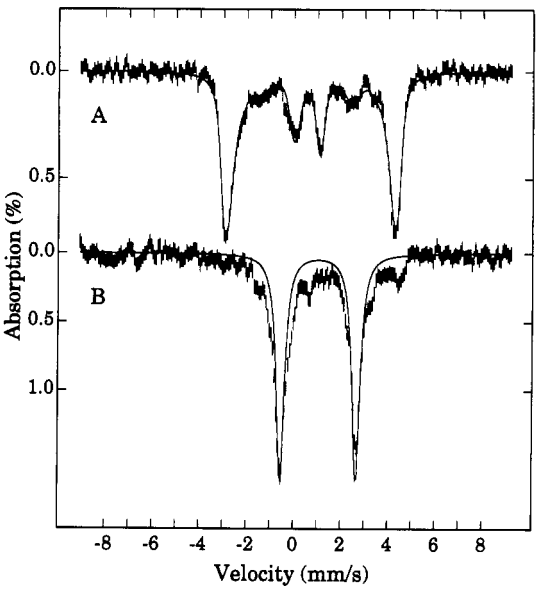

FIGURE 6: Mössbauer spectra of wild-type IPNS·ACV·NO complex and its photolyzed product. (A) Anaerobic IPNS·ACV·NO complex was prepared in parallel to that of Figure 5; (B) sample from (A) after exposure to white light (350–800 nm) in the Mössbauer cryostat at 4.2 K for 30 min. A quadrupole doublet of a diamagnetic species corresponding to 11% of spectrum A was subtracted from the data prior to computer simulations (see footnote 3). The solid line in (A) is a computer simulation based on the spin Hamiltonian of eq 3 using the parameters of Table II for the enzyme·NO·ACV complex. The solid line in (B) outlines the quadrupole doublet (approximately 75% of total iron) of the photolyzed IPNS·ACV complex. Spectra were obtained at 4.2 K in a 60-mT parallel field.

Table IV: ACV Analogue Binding to Wild-Type IPNS·NO[a]

analogue	optical λ_{max} (nm)	EPR (E/D)	K_i[b] (mM)
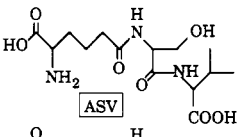 ASV	yellow, 430	0.017	>10
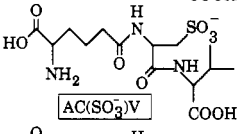 AC(SO_3^-)V	yellow, 430	0.013	0.90
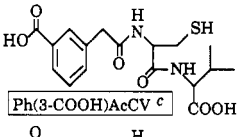 Ph(3-COOH)AcCV [c]	pink, 500	0.035	0.12
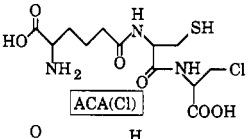 ACA(Cl)	pink, 500	0.030	0.14
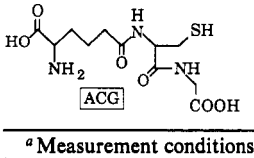 ACG	orange-red, 500 (shoulder)	0.030	0.12

[a] Measurement conditions are described in Experimental Procedures. [b] Inhibition was assumed to be of the competitive type. [c] Alternate substrate (Baldwin & Abraham, 1988).

Analogues. The proposed binding of the thiolate moiety of ACV to the active site Fe^{2+} was also examined using substrate analogues. Table IV summarizes the changes in the EPR and optical properties observed for the IPNS·NO complexes formed with several analogues. It was observed that the cysteinyl group is essential for retention of the spectroscopic properties characteristic of the IPNS·ACV·NO complex. For

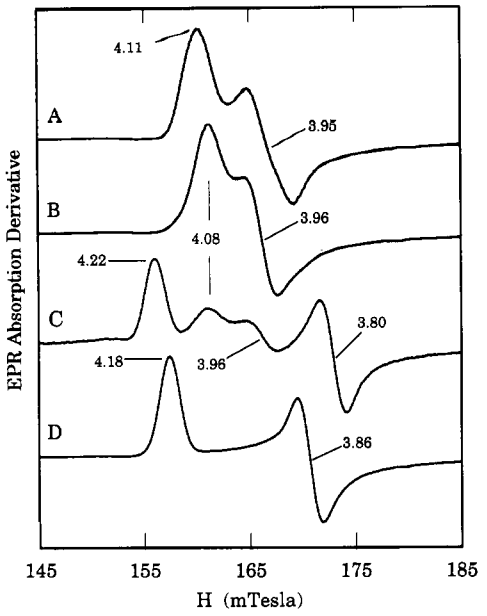

FIGURE 7: EPR spectra of wild-type IPNS·ACV analogue·NO complexes. (A) Enzyme (300 μM) plus 150 mM ASV plus NO. (B) Enzyme (300 μM) plus 10 mM AC(SO_3^-)V plus NO. (C) Enzyme (100 μM) plus 0.60 mM ACV plus NO to which 25 mM AC(SO_3^-)V was subsequently added. Prior to adding AC(SO_3^-)V, the EPR spectrum showed that only the IPNS·ACV·NO species was present. (D) Enzyme (300 μM) plus 100 mM ACA(Cl) plus NO. Instrumental conditions were as described in Figure 3.

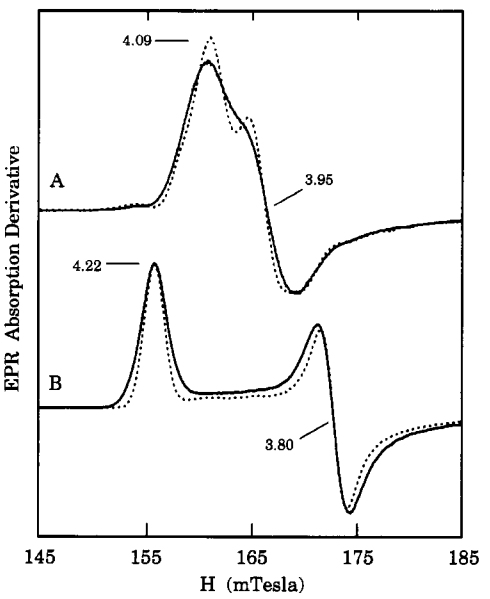

FIGURE 8: Hyperfine broadening of wild-type IPNS·NO complexes by ^{17}O-enriched water. IPNS (200 μM) in 100 mM MOPS buffer, pH 7.1, was lyophilized and rehydrated with either ^{17}O-enriched (—) or unenriched (---) water. (A) IPNS plus NO; (B) IPNS plus 5 mM ACV plus NO. In (A), the spectra are normalized to the same number of spins, while in (B) the spectra are normalized to the same signal intensity at $g = 4.22$ (^{17}O-enriched sample spectrum multiplied by 1.18) to better illustrate the hyperfine broadening. Instrumental conditions were as described in Figure 3.

example, ASV, in which a seryl group replaces the cysteinyl moiety, causes only minor changes in EPR line shape (compare Figures 3A and 7A) and no apparent changes in the optical spectrum. ASV does not inhibit the enzyme at concentrations as high as 20 times the K_M value of ACV, suggesting that it binds poorly to the active site. In contrast, the ACV analogue formed by oxidation of the ACV thiolate to sulfonate [AC(SO_3^-)V] is a very good competitive inhibitor (K_i = 0.9 mM), showing that the enzyme retains relatively high affinity for this analogue. Nevertheless, the spectral characteristics of the IPNS·[AC(SO_3^-)V]·NO complex are similar to those of IPNS·NO (Figure 7B, Table IV). As expected from the observed competitive inhibition, addition of a large excess of AC(SO_3^-)V to an IPNS·ACV·NO complex causes partial displacement of the ACV as shown by the appearance of the characteristic EPR spectrum with E/D = 0.013 (Figure 7C). Thus, an ACV analogue devoid of thiol can bind in the ACV binding site, but such analogues elicit none of the spectroscopic features characteristic of ACV binding.

ACV analogues in which the cysteine moiety is unaltered give markedly different results. These analogues elicit spectra very similar to those from the ACV complex. For example, the ACA(Cl) and ACG analogues, in which the terminal valine residue is changed to chloroalanine and glycine, respectively, are good inhibitors, and they cause changes in both the EPR and optical spectra analogous to those caused by ACV (Figure 7D and Table IV). Analogous results were observed for the Ph(3-COOH)AcCV analogue of ACV in which the adipoyl moiety is replaced by a (3-carboxyphenyl)acetyl group (Table IV). These results suggest that a substrate thiolate is essential for the formation of both an EPR species with an $E/D \approx 0.035$ and an optical spectrum exhibiting an absorption maximum near 510 nm.

Studies of Water Coordination. EPR-Detected ^{17}O-Enriched Water Hyperfine Broadening in Wild-Type IPNS·NO Complexes. The accessibility of the active site iron of IPNS to solvent was examined by preparing the enzyme–nitrosyl complex in ^{17}O-enriched water. The sharp $S = {}^3/_2$ EPR resonances of the IPNS·NO complex are broadened by nuclear hyperfine interaction with ^{17}O ($I = {}^5/_2$) as shown in Figure 8A. Due to the axial nature of the IPNS·NO complex EPR spectrum, the hyperfine broadening from the ^{17}O nucleus results in a merging of the two resonances near $g = 4$. The isolated resonances at $g = 4.22$ and 3.80 of the IPNS·ACV·NO complex are also broadened due to hyperfine interactions with ^{17}O-enriched water (Figure 8B). Control experiments showed that no shift or broadening of the EPR resonances occurred due to changes in pH between 6.5 and 7.5. Thus, water or hydroxide coordinates to the active site iron in both the substrate-free and ACV-complexed enzyme when NO is present.

Discussion

ACV Directly Coordinates to the Active Site Iron. We have shown here that mutated IPNS devoid of cysteine is spectroscopically indistinguishable from the wild-type enzyme. Moreover, the cysteine-free enzymes exhibit the same changes in the Mössbauer, EPR, and optical spectra on complexation with ACV or ACV *and* NO that we have previously associated with thiolate ligation in the wild-type IPNS·ACV complex (Chen et al., 1989). Together with the preceding EXAFS study (Scott et al., 1992), which indicates that sulfur is part of the iron coordination when ACV binds to the enzyme, these results clearly demonstrate that the thiolate moiety of ACV coordinates to the active site iron in the enzyme–substrate complex. Accordingly, only ACV analogues containing a central cysteinyl moiety elicit the characteristic spectroscopic changes. Although it is now clear that the endogenous cysteines do not coordinate to the iron, the decreased affinity of the mutated enzymes for ACV revealed by the Mössbauer spectra suggests that they do affect substrate binding. This may occur by directly or indirectly influencing the structure of the active site. Such effects would be in accord with the differences in kinetic parameters observed for the mutated enzymes (Samson et al., 1987; Kriauciunas et al., 1991).

Model for the Iron Site Ligation. The iron coordination of IPNS has been investigated by a variety of spectroscopic techniques. The results from these studies are all consistent with a 6-coordinate Fe^{2+} site with O- or N-type ligands for the uncomplexed enzyme (Ming et al., 1990, 1991; Scott et al., 1992). ^{1}H-NMR studies of Co^{2+}- and Fe^{2+}-reconstituted IPNS (Ming et al., 1990, 1991) further suggested that the endogenous ligands include an aspartate and 3 histidines. The presence of 2 or 3 histidine ligands is also indicated by multiple-scattering analysis of the EXAFS data presented in the preceding study (Scott et al., 1992). Moreover, ESEEM measurements of Cu^{2+}-reconstituted IPNS (Jiang et al., 1991) indicated 2 equatorial histidine ligands as well as water in the metal coordination sphere.

The nature of the Fe^{2+} coordination in the IPNS·ACV complex has been more difficult to ascertain due, in part, to the complications inherent in forming a uniform enzyme–substrate complex for an enzyme that binds substrate relatively weakly ($K_D \approx 18$ mM). The coordination of the ACV thiolate to the initially 6-coordinate iron center demonstrated here suggests that at least one of the original ligands is replaced. ESEEM measurements of the ACV complex of the Cu^{2+}-reconstituted enzyme (Jiang et al., 1991) have shown that a water is lost from the iron coordination upon ACV binding, suggesting that it may be directly displaced by the ACV thiolate. This conclusion was indirectly supported by the ^{1}H-NMR spectrum of the Fe^{2+}-containing IPNS·ACV complex partially saturated[7] with ACV (Ming et al., 1990, 1991), which was interpreted to indicate that none of the endogenous ligands of IPNS are lost when ACV binds (see further discussion of this conclusion below). However, the positions of several of the resonances associated with the ligands were shifted, suggesting that some reorganization of the site had occurred.

The binding of NO to IPNS was also observed to cause changes in the positions of ^{1}H-NMR resonances from the bound histidines (Ming et al., 1991). In addition, the resonances from the aspartate vanished. When ACV and NO were added together, resonances from the aspartate and one of the histidines disappeared. An unambiguous assessment of the iron coordination from these spectra is not possible, because failure to observe paramagnetically shifted NMR resonances can be ascribed to several factors including ligand dissociation, increased relaxation rates, or changes in structure that result in less unpaired spin density on the ligand. Nevertheless, additional insight into the effect of NO and ACV binding on the iron coordination can be gained by further consideration of these results in light of the results presented here.

The current study shows that at least three iron coordination sites can be simultaneously occupied by *exogenous* ligands in the IPNS·ACV·NO complex (ACV, water, and NO). Provided that the iron is maximally 6-coordinate, these results suggest that the iron has no more than 3 *endogenous* ligands in this complex. The photodissociated product of this complex exhibits a Mössbauer spectrum which is very similar to that of IPNS·ACV. Since NO is photodissociated at 4 K, a temperature at which protein structural changes to allow rebinding of endogenous ligands would be severely restricted, this observation raises the possibility that the IPNS·ACV complex is 5-coordinate and has the same three endogenous ligands as IPNS·ACV·NO. However, rebinding of a weak, mobile ligand in the NO ligation site cannot be ruled out, so long as it does not appreciably affect the Mössbauer spectrum. Consequently, these results suggest that the coordination of NO to the IPNS·ACV complex involves the displacement of at most one ligand. In the context of the current studies, then, it is likely that the loss of ^{1}H-NMR resonances from two endogenous ligands of the active site iron in the IPNS·ACV·NO complex is due to causes other than ligand dissociation for at least one of these ligands. Since addition of NO in the absence of ACV causes only the aspartate resonance to disappear, it seems reasonable that aspartate is the dissociating ligand and that the loss of histidine resonances in the IPNS·ACV·NO complex is due to reorientation or relaxation effects. Unfortunately, this determination cannot be made with certainty, and the opposite proposal has been forwarded on the basis of chemical arguments developed from model studies (Ming et al., 1991). It must be noted, however, that NO appears to have a special, sequestered binding site in IPNS as well as several other mononuclear Fe^{2+}-containing enzymes (Arciero et al., 1985; Harpel & Lipscomb, 1990a,b) which may be integral to their mechanisms (see discussion below); thus conclusions drawn from model studies must be interpreted with caution.

It is interesting to note that analysis of the X-ray absorption edge structure presented in the preceding study (Scott et al., 1992) shows that a major change in the Fe^{2+} coordination occurs upon ACV binding and that the position and intensity of the edge features are between those characteristic of 5- and 6-coordination. This observation supports the implication of the photodissociation results discussed above that ACV binding to IPNS results in the displacement of both a solvent and one of the endogenous ligands from the iron, leaving the iron 5-coordinate (or 6-coordinate with a weak sixth ligand). This possibility appears to conflict with the NMR results which indicate that all four of the NMR-detectable endogenous ligands are retained when ACV binds (Ming et al., 1990, 1991). However, a probable lack of substrate saturation in the relevant NMR sample disallows direct comparison of the results.[7] If the binding of ACV does cause the iron to become 5-coordinate, there would be no need to invoke further ligand dissociation when NO binds, thus accounting for the nearly identical Mössbauer spectra of the IPNS·ACV complexes produced by simple equilibration of IPNS with ACV and by photodissociation of IPNS·ACV·NO.

Another possible means to reconcile the NMR and photodissociation results is to assume that the structural changes attendant to ACV binding cause the aspartate to be repositioned so that its bond to the iron is weakened, thus allowing facile displacement by NO. Such a change would readily account for the alteration in the NMR spectrum, and the weak oxygen ligand would not be expected to greatly influence either the quadrupole splitting or the isomer shift of the Mössbauer spectrum. Consequently, the spectrum of the IPNS·ACV complex formed by photodissociation might strongly resemble that from the complex formed by equilibration of IPNS and ACV. The model for the active site which has developed from the results reported here and the other spectroscopic studies is summarized in Scheme II.

Implications for the Mechanism of IPNS. The occupancy of three iron ligand sites by exogenous ligands has precedence in the active site Fe^{2+} coordination of extradiol-cleaving catecholic dioxygenases (Arciero et al., 1985; Arciero &

[7] The NMR sample of the IPNS·ACV complex used to make the NMR measurements (Ming et al., 1990, 1991) contained only 5 mM ACV, which, based on the results presented here, is significantly below the concentration required to saturate the samples ($K_D \approx 18$ mM). Thus, the relevance of the NMR data for this particular sample cannot be unambiguously ascertained. In contrast, the NMR sample of the IPNS·ACV·NO complex, in all likelihood, did represent a uniform sample despite the similarly low concentration of ACV because binding of NO greatly decreases the K_D for ACV (see Figures 2C,D and 6A).

Scheme II: Proposal for the Active Site Fe^{2+} Ligand Structure of IPNS in Complexes with NO and Substrate[a]

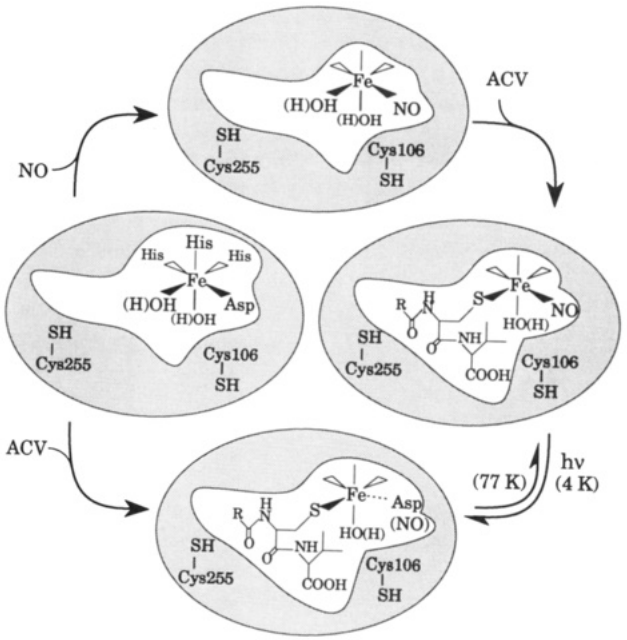

[a] The relative positions of the ligands are arbitrary, and three histidine ligands are assumed to be present in each complex. It is unlikely that NO leaves the protein matrix following photodissociation from the IPNS·ACV·NO complex because it readily reassociates at 77 K. The substrate complexes formed by photodissociation of the IPNS·ACV·NO complex and by simple addition of ACV to the resting enzyme are represented by one structure due to the similarity of their Mössbauer spectra. However, addition of a weak sixth ligand in the complex formed by simple addition would not be inconsistent with the data (see text).

Lipscomb, 1986) and gentisate 1,2-dioxygenase (Harpel & Lipscomb, 1990a,b) which catalyze ring opening reactions of aromatic substrates by insertion of both atoms of oxygen from O_2. In contrast, enzymes such as lipoxygenase, which apparently do not bind the substrate directly to the iron, have only one site that can bind either H_2O or NO, but not both simultaneously (Nelson, 1987, 1988). Like IPNS, the Fe^{2+} dioxygenases energetically couple the binding of NO and of organic substrate so that the binding of one facilitates the other (Arciero et al., 1985). We have proposed that in the case of the extradiol dioxygenases this provides a mechanism to ensure that both substrates are present at the same time within the enzyme active site (Arciero & Lipscomb, 1986; Harpel & Lipscomb, 1990b). Briefly, the binding of anionic substrate ligands to the iron (catecholate in the case of the catecholic dioxygenases) lowers the redox potential of the iron, thereby increasing the affinity for electrophilic ligands such as O_2 and NO (an O_2 analogue). A similar mechanism could readily be envisioned for IPNS in which substrate thiolate ligation initiates catalysis by promoting O_2 binding in another iron ligand site. Subsequent catalytic steps of the dioxygenase and IPNS mechanisms clearly diverge, and the fate of O_2 is different. Nevertheless, the crucial roles of iron in the assembly of the substrates in close proximity, and the promotion of electron transfer between them to initiate catalysis, may be similar.

The iron coordinations of the Fe^{2+} dioxygenases and IPNS also differ in the fate of the coordinated water (or hydroxide) upon substrate binding. In contrast to the results presented here for IPNS·NO complexes, all of the water detected in the substrate-free nitrosyl complex of the dioxygenases is apparently displaced as substrate forms a bidentate complex with the iron (Arciero & Lipscomb, 1986; Harpel & Lipscomb, 1990b). It is conceivable, albeit unlikely, that the bound water is utilized at some point in IPNS catalysis or serves to stabilize an activated oxygen intermediate. Alternatively, the water may be displaced by an atom from ACV other than the thiolate at some later stage during the reaction as a precursor to strained ring formation [see, for example, Baldwin and Abraham (1988)]. In the case of the dioxygenases, we have proposed that a departing hydroxide may act as a base to promote deprotonation of the substrate aromatic hydroxyl groups required for catalysis (True et al., 1990). As discussed above, one water, presumably bound as hydroxide, may serve this function in IPNS as the ACV thiol is deprotonated in binding to the active site iron. Similar considerations may apply to the water that remains bound to the iron in the ACV complex as a means to promote specific ring closure in later steps of the IPNS mechanism.

The oxygen stoichiometry and the stereochemical course of the reactions catalyzed by IPNS with ACV analogues have led Baldwin and Abraham (1988) to propose a variety of mechanisms in which the initial β-lactam ring closure is coupled to 2-electron reduction of O_2 via simultaneous formation of Fe^{2+}–ACV thiolate and Fe^{2+}–O_2 bonds. This implies fissure of the O–O bond and release of H_2O by analogy with the mechanisms proposed for cytochrome P450 (McMurry & Groves, 1986), peroxidases [see, for example, Andersson and Dawson (1990)], and methane monoxygenase (Fox et al., 1990). The resulting iron-bound activated oxygen atom could conceivably either be transferred to a substrate in oxygenase-like chemistry or initiate the thiazolidine ring closure reaction depending upon the chemical nature of the ACV analogue present in the active site. The spectroscopic studies presented here show that simultaneous occupancy of iron coordination sites by ACV thiolate and the oxygen-like molecule NO can occur, in accord with this mechanistic proposal.

Acknowledgments

We thank Dr. Robert A. Scott for many useful discussions and suggestions in the preparation of the manuscript.

References

Aasa, R., & Vänngård, T. (1975) *J. Magn. Reson. 19*, 308–315.

Andersson, L. A., & Dawson, J. H. (1990) *Struct. Bonding 74*, 1–40.

Arciero, D. M., & Lipscomb, J. D. (1986) *J. Biol. Chem. 261*, 2170–2178.

Arciero, D. M., Lipscomb, J. D., Huynh, B. H., Kent, T. A., & Münck, E. (1983) *J. Biol. Chem. 258*, 14981–14991.

Arciero, D. M., Orville, A. M., & Lipscomb, J. D. (1985) *J. Biol. Chem. 260*, 14035–14044.

Austin, R. H., Beeson, K. W., Eisenstein, L., Frauenfelder, H., & Gunsalus, I. C. (1975) *Biochemistry 14*, 5355–5373.

Baldwin, J. E., & Abraham, E. P. (1988) *Nat. Prod. Rep. 5*, 129–145.

Baldwin, J. E., & Bradley, M. (1990) *Chem. Rev. 90*, 1079–1088.

Baldwin, J. E., Killin, S. J., Pratt, A. J., Sutherland, J. D., Turner, N. J., Crabbe, M. J. C., Abraham, E. P., & Willis, A. C. (1987) *J. Antibiot. 40*, 652–659.

Baldwin, J. E., Coates, J. B., Moloney, M. G., Pratt, A. J., & Willis, A. C. (1990) *Biochem. J. 266*, 561–567.

Blumberg, W. E. (1967) in *Magnetic Resonance in Biological Systems* (Ehrenberg, A., Malmstrom, B. G., & Vånngård, T., Eds.) pp 119–133, Pergamon Press, New York.

Blumberg, W. E., & Peisach, J. (1973) *Ann. N.Y. Acad. Sci. 222*, 539–560.
Boelens, R., Rademaker, H., Pel, R., & Wever, R. (1982) *Biochim. Biophys. Acta 679*, 84–94.
Carr, L. C., Skatrud, P. L., Scheetz, M. E.; Queener, S. W., & Ingolia, T. D. (1986) *Gene 48*, 257–266.
Castro, J. M., Libras, P., Laîz, L., Crotês, J., & Martîn, J. F. (1988) *J. Gen. Microbiol. 134*, 133–141.
Champion, P. M., Lipscomb, J. D., Münck, E., Debrunner, P., & Gunsalus, I. C. (1975) *Biochemistry 14*, 4151–4158.
Chen, V. J., Orville, A. M., Harpel, M. R., Frolik, C. A., Surerus, K., Münck, E., & Lipscomb, J. D. (1989) *J. Biol. Chem. 264*, 21677–21681.
Fox, B. G., Borneman, J. G., Wackett, L. P., & Lipscomb, J. D. (1990) *Biochemistry 29*, 6419–6427.
Harpel, M. R., & Lipscomb, J. D. (1990a), *J. Biol. Chem. 265*, 6301–6311.
Harpel, M. R., & Lipscomb, J. D. (1990b) *J. Biol. Chem. 265*, 22187–22196.
Hirs, C. H. W. (1967) *Methods Enzymol. 11*, 197–199.
Ingraham, L. L., & Meyer, D. L. (1985) *Biochemistry of Dioxygen*, pp 139–246, Plenum Press, New York.
Jiang, F., Peisach, J., Ming, L.-J., Que, L., Jr., & Chen, V. J. (1991) *Biochemistry 30*, 11437–11445.
Kent, T., Spartalian, K., Lang, G., & Yonetani, T. (1977) *Biochim. Biophys. Acta 490*, 331–340.
Kriauciunas, A., Frolik, C. A., Hassel, T. C., Skatrud, P. L., Johnson, M. G., Holbrook, N. L., & Chen, V. J. (1991) *J. Biol. Chem. 266*, 11779–11788.
Lang, G. (1970) *Q. Rev. Biophys. 3*, 1–60.
Leskiw, B. K., Aharonowitz, Y., Mevarech, M. Wolfe, S., Vining, L. C., Westlake, D. W., & Jensen, S. E. (1988) *Gene 62*, 187–196.
Lipscomb, J. D. (1980) *Biochemistry 19*, 3590–3599.
Lipscomb, J. D., & Orville, A. M. (1992) in *Metal Ions in Biological Systems* (Sigel, H., & Sigel, A., Eds.) Vol. 28, pp 243–298, Marcel Dekker, New York.
McMurry, T. J., & Groves, J. T. (1986) in *Cytochrome P-450 Structure, Mechanism, and Biochemistry* (Ortiz de Montellano, P. R., Ed.) pp 1–28, Plenum Publishing Corp., New York.
Miller, J. R., & Ingolia T. D. (1989) *Mol. Microbiol. 3*, 689–695.
Ming, L.-J., Que, L., Jr., Kriauciunas, A., Frolik, C. A., & Chen, V. J. (1990) *Inorg. Chem. 29*, 1111–1112.
Ming, L.-J., Que, L., Jr., Kriauciunas, A., Frolik, C. A., & Chen, V. J. (1991) *Biochemistry 30*, 11653–11659.
Nelson, M. J. (1987) *J. Biol. Chem. 262*, 12137–12142.
Nelson, M. J. (1988) *J. Am. Chem. Soc. 110*, 2985–2986.
Palissa, H., von Dõhren, H., Klinekauf, H., Ting, H.-H., & Baldwin, J. E. (1989) *J. Bacteriol. 171*, 5720–5728.
Pang, C.-P., Chakravarti, B., Adlington, R. M., Ting, H.-H., White, R. L., Jayatilake, G. S., Baldwin, J. E., & Abraham, E. P. (1984) *Biochem. J. 222*, 789–795.
Ramon, D., Carramolino, L., Patino, C., Sanchez, F., & Penalva, M. A. (1987) *Gene 57*, 171–181.
Samson, S. M., Belagaje, R., Blankenship, D. T., Chapman, J. L., Perry, D., Skatrud, P. L., Van Frank, R. M., Abraham, E. P., Baldwin, J. E., Queener, S. W., & Ingolia, T. D. (1985) *Nature 318*, 191–194.
Samson, S. M., Chapman, J. L., Belagaje, R., Queener, S. W., & Ingolia, T. D. (1987) *Proc. Natl. Acad. Sci. U.S.A. 84*, 5705–5709.
Scholes, C. P., Isaacson, R. A., Yonitoni, T., & Feher, G. (1973) *Biochim. Biophys. Acta 322*, 457–462.
Scott, R. A., Wang, S., Eidsness, M. K., Kriauciunas, A., Frolik, C. A. & Chen, V. J. (1992) *Biochemistry* (preceding paper in this issue).
Sharrock, M., Münck, E., Debrunner, P. G., Marshall, V., Lipscomb, J. D., & Gunsalus, I. C. (1973) *Biochemistry 12*, 258–265.
Shiffman, D., Mevarech, M., Jensen, S. E., Cohen, G., & Aharanowitz, Y. (1988) *Mol. Gen. Genet. 214*, 562–569.
True, A. E., Orville, A. M., Pearce, L. L., Lipscomb, J. D., & Que, L., Jr. (1990) *Biochemistry 29*, 10847–10854.
Weigel, B. J., Burgett, S. G., Chen, V. J., Skatrud, P. L., Frolik, C. A., Queener, S. W., & Ingolia, T. D. (1988) *J. Bacteriol. 170*, 3817–3826.
White, R. L., John, E. M. M., Baldwin, J. E., & Abraham, E. P. (1982) *Biochem. J. 203*, 791–793.
Whittaker, J. W., & Lipscomb, J. D. (1984) *J. Biol. Chem. 259*, 4476–4486.
Whittaker, J. W., Lipscomb, J. D., Kent, T. A., & Münck, E. (1984) *J. Biol. Chem. 259*, 4466–4475.
Whittaker, J. W., Orville, A. M., & Lipscomb, J. D. (1990) *Methods Enzymol. 188*, 82–88.
Yoshida, S., Hori, H., & Orii, Y. (1980) *J. Biochem. 88*, 1623–1627.